09

Study of the low-order mode field structure impact on Y-splitter parameters in photonic integrated circuits

© P.V. Volkov[1], O.S. Vyazankin[1], A.I. Bobrov[2], A.V. Nezhdanov[2], D.A. Semikov[1], K.V. Sidorenko[2]

[1] Institute of Physics of Microstructures, Russian Academy of Sciences, Nizhny Novgorod, Russia
[2] Lobachevsky State University, Nizhny Novgorod, Russia
E-mail: volkov@ipmras.ru

Received January 21, 2025
Revised July 2, 2025
Accepted July 4, 2025

The impact of low-order mode operation in silicon integrated waveguides on the performance of Y-splitters with a rib geometry, fabricated on a silicon-on-insulator (SOI) platform, is investigated. It is demonstrated that the TE_{10} mode, emerging when a standard 500×220 nm channel silicon waveguide is overgrown with silicon oxide, significantly alters the Y-splitter characteristics. As a result, the splitting ratio becomes dependent on the relative alignment between the optical fiber delivering light to the photonic integrated circuit and the input coupling structure.

Keywords: rib waveguides, channel waveguides, integrated splitters.

DOI: 10.61011/TPL.2025.10.62106.20261

Photonic integrated circuits (PICs) have advanced rapidly in recent years [1]. They are regarded as possible building blocks for complex optical circuits and active devices. Of particular interest is silicon photonics (specifically, silicon-on-insulator (SOI) PICs), since such components may be produced using technological processes that are standard for silicon electronics.

Silicon waveguides of two geometries are commonly used at present: rectangular waveguides (fully etched) and rib ones, where the top layer of silicon is etched to a shallow depth (60–80 nm) and a rib is shaped to localize radiation and form a waveguide channel underneath it. The main advantage of fully etched channel waveguides is the high mode localization induced by a high optical contrast between the waveguide material (the refraction index of silicon at a wavelength of $1.55\,\mu$m is 3.44) and the substrate material (the refraction index of SiO_2 is 1.44), which allows the waveguide to be bent with bending radii of a few micrometers. The rib geometry is more complex from a manufacturing standpoint, since it requires additional lithography with stringent requirements as to the accuracy of alignment between layers, but it offers a number of advantages. First, rib waveguides have significantly lower propagation losses, which is attributable to a smaller side wall area and, consequently, less pronounced scattering of a propagating wave [2]. Second, the rib geometry is characterized by a significantly lower sensitivity of splitter parameters to the technological spread of lateral dimensions [3]. Therefore, a hybrid approach with the rib geometry used for long linear sections and splitters and the channel geometry with converters used at bends is the optimum one in terms of miniaturization, minimization of losses, and reproducibility of parameters.

The standard size of a fully etched SOI waveguide is 500×220 nm [4]. These dimensions ensure single-mode radiation propagation and are suitable for manufacturing processes with fairly lenient design rules (e.g., an inexpensive and accessible 350 nm process). However, when such a waveguide is overgrown with silica, which is often needed to insulate the control PIC layers, the TE_{10} mode starts to propagate alongside with the fundamental TE_{00} mode, inducing parasitic effects.

Radiation splitters are one of the key PIC elements, since they are the ones shaping the circuit topology. Deviation of their parameters from the designed values may exert a critical influence on the operation of the entire PIC. Three main designs may be distinguished [5]: a directional coupler, a multimode interferometer splitter, and a Y-splitter. The first two types allow for an arbitrary splitting ratio, while a Y-splitter provides even splitting and is used, in particular, to construct PIC interferometers. In the present study, the influence of mode TE_{10} on the parameters of a rib Y-splitter with fully etched feeder waveguides was investigated theoretically and experimentally. Multimode operation of Si waveguides has already been examined earlier (e.g., in [6]), but the parasitic effects of intermode interaction in rib waveguide splitters have not been considered.

The geometry of the modeled splitter built based on rib waveguides is shown in Fig. 1. Figure 1, *a* shows the complete diagram of the splitter with input and output diffraction gratings, and Fig. 1, *b* presents an electron microscope image of the fabricated sample. The rib height was 70 nm, its width was 500 nm, the pedestal width was 500 nm on each side of the rib, and the waveguide divergence angle was 4°. Radiation was supplied to the Y-splitter via fully etched channel waveguides with a width

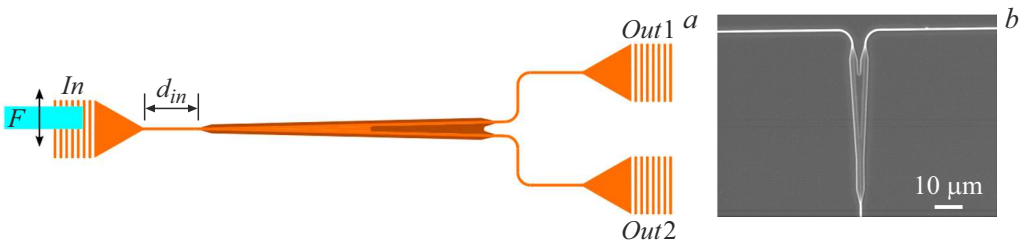

Figure 1. *a* — *Y*-splitter diagram. *F* — optical fiber, *In* — splitter input, *Out*1, 2 — splitter outputs, and d_{in} — input waveguide length. *b* — Electron micrograph of the sample.

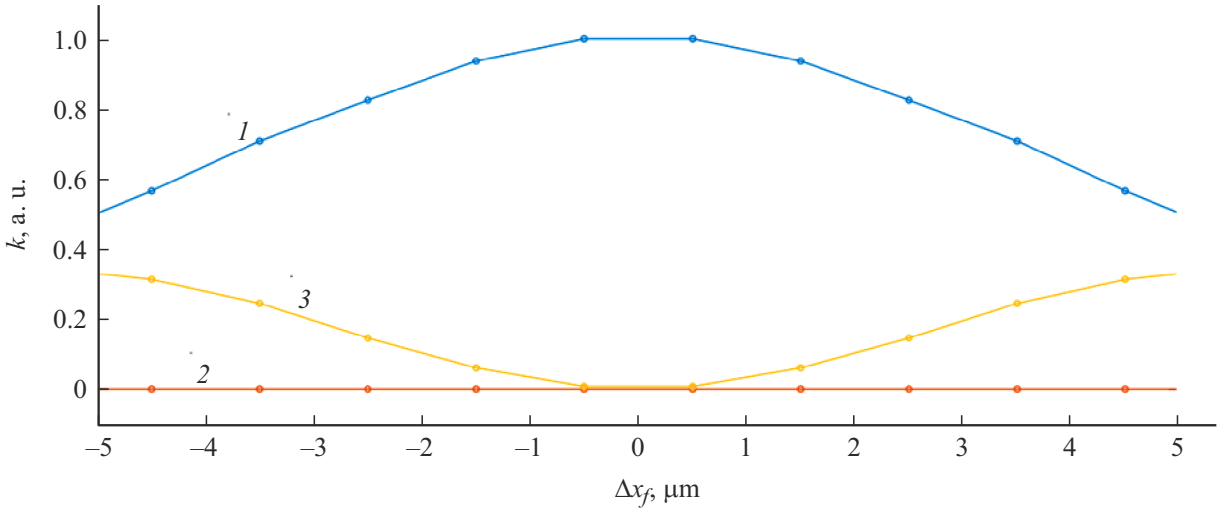

Figure 2. Dependences of the mode excitation coefficients on the source position relative to the input diffraction grating. *1* — TE_{00}, *2* — TM_{00}, and *3* — TE_{10}.

of 500 nm and a height of 220 nm. Matching tapers were formed at the input and outputs of the splitter. The entire surrounding space was filled with silica.

Modeling was performed in the ANSYS Lumerical package at a wavelength of 1550 nm. A variable-step grid with a smaller step (approximately $\lambda/50$) in the region of waveguides and boundaries and a larger step (approximately $\lambda/20$) in the free space (λ is the wavelength of light in the waveguide) was used. Two problems were solved: (1) obtaining the dependence of the relative excitation coefficients of modes TE_{00}, TE_{10}, and TM_{00} on the position of the optical fiber (*F* in Fig. 1) relative to the input grating (Fig. 2); (2) obtaining the dependence of the splitting ratio of the *Y*-splitter under consideration on the phase shift and the ratio of amplitudes of modes TE_{00} and TE_{10} (Fig. 3).

Radiation incident on the grating had a Gaussian profile and linear polarization, and oscillation of the electric field vector was aligned with grating grooves. It can be seen from Fig. 2 that the power ratio of modes TE_{00} and TE_{10} changes significantly when the excitation source is shifted away from the center of the grating. Since modes TE_{00} and TE_{10} have different propagation constants, the phase shift between them at the splitter input is determined by length d_{in} of the feeder waveguide (Fig. 1). It is also evident from Fig. 2 that the excitation coefficient of the TM_{00} mode is zero at any position of the optical fiber, which is attributable to orthogonality of polarization of the TE and TM modes and allows one to exclude it from calculations.

To find the calculated dependence of the splitting ratio on the ratio of amplitudes and phases of modes, a mode source, which could set an arbitrary ratio of amplitudes and phases of excited modes, was installed at the splitter input. Two modes were excited: TE_{00} and TE_{10}.

Figure 3 shows a series of plots illustrating the dependence of power division at the *Y*-splitter output on the phase difference between modes TE_{00} and TE_{10} at different ratios of their powers. Let us introduce two parameters for convenience: γ and φ ($\gamma = P_{TE_{10}}/P_{TE_{00}}$, where $P_{TE_{00}}$ is the power of mode TE_{00} and $P_{TE_{10}}$ is the power of mode TE_{10}; φ is the phase shift between these modes at the splitter input). Let us also introduce transmission ratios

$$T_{11} = P_{out1}/P_{in}, \qquad T_{12} = P_{out2}/P_{in},$$

where P_{in} is the total optical power at the splitter input and $P_{out1,2}$ is the total power at outputs 1 and 2, respectively.

It is evident from Fig. 3 that the phase shift between modes has a profound influence on the splitting ratio, and the ratio of amplitudes sets the contrast of splitting

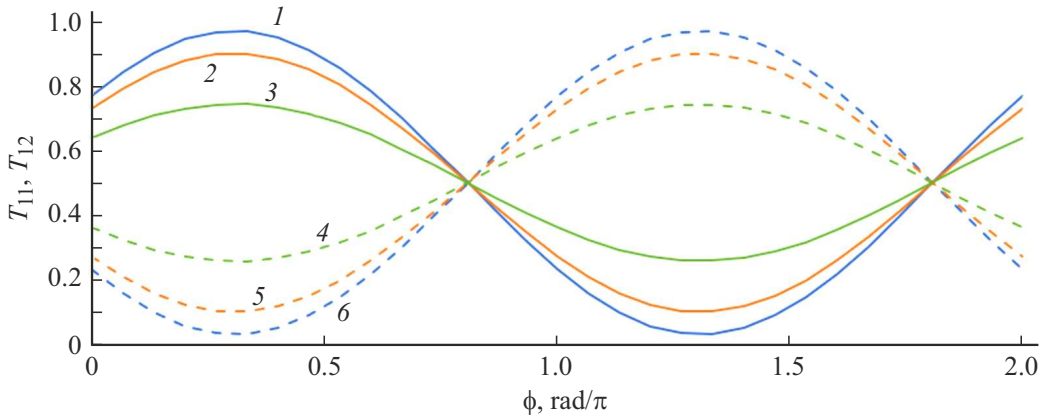

Figure 3. Dependences of the optical power transmission coefficients in a rib Y-splitter on the phase difference between TE_{00} and TE_{10} at different ratios of their amplitudes. *1* — T_{11}, $\gamma = 1$; *2* — T_{11}, $\gamma = 0.5$; *3* — T_{11}, $\gamma = 0.25$; *4* — T_{12}, $\gamma = 0.25$; *5* — T_{12}, $\gamma = 0.5$; *6* — T_{12}, $\gamma = 1$.

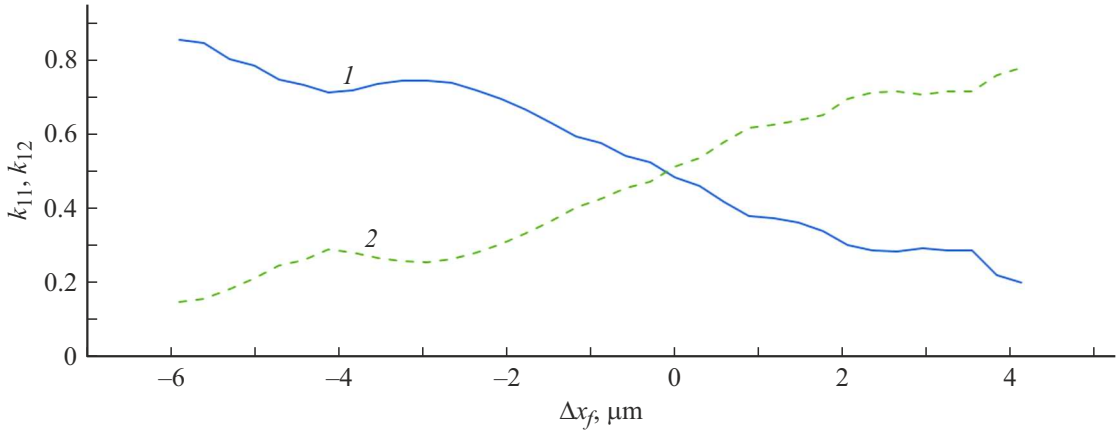

Figure 4. Dependences of the splitting ratios of the Y-splitter on the source position relative to the input diffraction grating. *1* — k_{11}; *2* — k_{12}.

unevenness. This effect arises due to the antisymmetric nature of the transverse phase profile of mode TE_{10}, which leads to the formation of an asymmetric field distribution at the Y-splitter input that depends on the ratio of amplitudes and phases of the modes under consideration.

A Y-splitter of the examined geometry was fabricated in order to verify this reasoning experimentally (Fig. 1, *b*). Light from an optical fiber was coupled into the integrated circuit via a diffraction grating and a 200-μm-long adiabatic taper [7]. The shift of the optical fiber across the grating could be controlled by the ratio of amplitudes of TE_{00} and TE_{10}: when the fiber was oriented centrally, the power was fed primarily into the TE_{00} mode, while the fiber displacement along the grating grooves (i.e., transverse to the waveguide axis) resulted in the emergence of an electric field distribution asymmetrical relative to the waveguide axis, which led to excitation of the TE_{10} mode.

The intensity at the splitter outputs was measured with an IR camera, which allowed us to image the beam at both splitter outputs simultaneously. The fiber was moved using a precision manual Luminos positioner with a step of 0.3 μm. Displacement range Δx_f of the fiber was 10 μm. The resulting image was processed, and the intensity ratio of beams was evaluated. Coefficients

$$k_{11} = I_1/(I_1 + I_2), \qquad k_{12} = I_2/(I_1 + I_2),$$

where $I_{1,2}$ are the measured beam intensities at outputs 1 and 2, respectively (in relative units), were calculated. The measurement results are shown in Fig. 4.

Figure 4 makes it clear that even splitting is achieved when the optical fiber is positioned near the center of the grating (i.e., on the waveguide axis), while its shift away from the waveguide axis translates into a large difference in the distribution of the optical radiation power at the splitter outputs.

Thus, the influence of violation of the single-mode regime, which is observed in standard 500 × 220 nm silicon waveguides overgrown with silica, on the operation of a rib Y-splitter was demonstrated theoretically and experimentally. It was found that excitation of the TE_{10} mode

exerts a considerable effect on the operating parameters of the element. To ensure single-mode operation of a 220-nm-high silica-covered waveguide, its width must be reduced, which necessitates the transition to significantly more stringent design rules. Mode filters, the simplest of which are *S*-shaped waveguide sections, may be used to minimize this effect.

Funding

Mathematical modeling was supported by the Ministry of Science and Higher Education of the Russian Federation (project No. FSWR-2022-0007). Experiments were performed as part of the research program of the National Center of Physics and Mathematics (topic No. 1 „National Center for Supercomputer Architecture Studies. Phase 2023–2025“).

Conflict of interest

The authors declare that they have no conflict of interest.

References

[1] S. Pai, Z. Sun, T.W. Hughes, T. Park, B. Bartlett, I.A.D. Williamson, M. Minkov, M. Milanizadeh, N. Abebe, F. Morichetti, A. Melloni, S. Fan, O. Solgaard, D.A.B. Miller, Science, **380** (6643), 398 (2023). DOI: 10.1126/science.ade84
[2] D. Melati, A. Melloni, F. Morichetti, Adv. Opt. Photon., **6** (2), 156 (2014). DOI: 10.1364/AOP.6.000156
[3] X. Liu, Y. Zhao, Z. Sheng, F. Gan, IEEE Photon. Technol. Lett., **36** (10), 637 (2024). DOI: 10.1109/LPT.2024.3381826
[4] S.K. Selvaraja, P. Sethi, *Review on optical waveguides* (InTech, 2018). DOI: 10.5772/intechopen.77150
[5] L. Zheng, Y. Chen, Z. Xue, J. Huang, M. Zhu, L. Wang, Optoelectron. Lett., **20**, 577 (2024). DOI: 10.1007/s11801-024-3258-3
[6] C. Li, D. Liu, D. Dai, Nanophotonics, **8** (2), 227 (2019). DOI: 10.1515/nanoph-2018-0161
[7] R. Marchetti, C. Lacava, L. Carroll, K. Gradkowski, P. Minzioni, Photon. Res., **7**, 201 (2019). DOI: 10.1364/PRJ.7.000201

Translated by D.Safin